GEOLOGICAL SURVEY OF CANADA
PAPER 89-16

ISOSTATIC AND ENHANCED ISOSTATIC GRAVITY ANOMALY MAPS OF THE ARCTIC

L.W. Sobczak
J.F. Halpenny

1990

Energy, Mines and Resources Canada
Énergie, Mines et Ressources Canada

Canada

GEOLOGICAL SURVEY OF CANADA
PAPER 89-16

ISOSTATIC AND ENHANCED ISOSTATIC GRAVITY ANOMALY MAPS OF THE ARCTIC

L.W. Sobczak
J.F. Halpenny

1989

Available in Canada through

authorized bookstore agents and other bookstores

or by mail from

Canadian Government Publishing Centre
Supply and Services Canada
Ottawa, Canada K1A 0S9

and from

Geological Survey of Canada offices:

601 Booth Street
Ottawa, Canada K1A 0E8

3303-33rd Street N.W.,
Calgary, Alberta T2L 2A7

A deposit copy of this publication is also available for
reference in public libraries across Canada

Cat. No. M44-89/16
ISBN 0-660-55068-7

Price subject to change without notice

Critical readers:
M. Drury
M. Thomas

Original manuscript submitted: 1988-06-08
Final version approved for publication: 1989-02-27

CONTENTS

Illustrations

ISOSTATIC AND ENHANCED ISOSTATIC GRAVITY ANOMALY MAPS OF THE ARCTIC

Abstract

Isostatic and enhanced isostatic gravity anomaly maps have been developed as aids for the interpretation of gravity anomalies with respect to geology. Isostatic gravity anomalies in the Arctic display topographic correlations which have been removed to produce a new type of gravity anomaly map – an enhanced isostatic map. This map enhances local, short-wavelength variations in gravity related to geological structures and eliminates those long-wavelength variations related to topographic, thermal and glacial effects. An enhanced isostatic anomaly map readily outlines active (tectonic) and inactive (stable) areas which can reflect the hydrocarbon potential of a sedimentary basin and indicates regions of young (usually < 100 Ma) oceanic and older (> 100 Ma) continental crust.

INTRODUCTION

A gravity database comprising 355 120 randomly distributed observations was used to generate a 1:6 000 000 scale map showing Bouguer anomalies on land and free-air anomalies offshore for the region north of 64°N latitude (Sobczak et al., in press). The observations are generally accurate to within 5 mGal for ice-free ocean areas and 2 mGal for most land and ice-covered ocean areas. This database has been reduced to 90 095 gridded (10 km interval) observations which have been used to produce separate Bouguer and free-air anomaly maps covering both land and ocean areas. Significant correlations between both Bouguer and free-air anomalies and elevations, or equivalent rock topography in cases of water or ice-capped regions, are noted (Fig. 1). This topographic influence tends to distort and/or obscure geological gravity signatures. For the conterminous United States such effects are largely removed by applying isostatic corrections (Simpson et al., 1986); a resulting isostatic anomaly map has limited correlation with topography. For the Arctic, however, correlations are evident, even between isostatic anomalies and elevation (Fig. 2). This remaining topographic component of the gravity field has been removed from the isostatic anomaly (IA) map to produce a new type of gravity anomaly map, – an enhanced isostatic anomaly map (EIA). Both the isostatic anomaly map and the enhanced isostatic anomaly map for the Arctic region (Maps 1738A and 1739A respectively,) are presented and described in this report.

The merits of the enhanced isostatic anomaly map were discussed briefly by Sobczak and Halpenny (in press). The enhanced isostatic anomaly map enhances variations in gravity related to geological structure, and eliminates those variations related to continental-oceanic crustal boundaries, water-rock interfaces and topography/bathymetry and associated isostatic roots/antiroots. Generally, the enhanced isostatic zero anomaly contour outlines areas of mafic volcanism and intrusion, oceanic or continental crust, and regions that have been tectonically active during the last 100 Ma. Within an oceanic region negative anomalies may indicate older (> 100 Ma) oceanic crust or pieces of continental crust, whereas positive anomalies indicate relatively new oceanic crust (< 100 Ma). Within a continental region, positive anomalies correspond with recently (< 100 Ma) active areas as indicated by mountains, volcanism, intrusions and uncompensated sedimentary loads, whereas negative anomalies indicate stable, older (> 100 Ma) areas and unmetamorphosed sedimentary basins which, in the Arctic, may have hydrocarbon potential.

GRAVITY DATA BASE

Initially, for the Bouguer anomaly map, an interpolation distance of 200 km between known gravity values was used, but this created several anomalous areas where no gravity observations had been made. For example, such areas were found north of the Chukchi Borderland, mountainous terrains of Ellesmere and Devon islands, northern Greenland, and the east and west sides of Iceland. As a result, a smaller (60 km) interpolation distance was used in these maps which removed most of these discrepancies. It created a map with many more holes in it but is a little more representative of the gravity data where gravity and either depth or elevation observations were made. Over the ocean, however, some areas may be covered by gravity observations with no corresponding water depths. This allows a free-air anomaly map to be determined but not a corresponding Bouguer anomaly map. Water depths could be interpolated from existing bathymetric charts to increase the coverage, but this was not done here due to lack of resources. Areas on the map where no gravity observations were made may not be representative of the gravity field.

GRAVITY ANOMALIES

Gravity anomalies were calculated from the following relationships:

free-air anomaly $FA = g_0 - \gamma_0 + Fe$

and Bouguer anomaly $BA = FA - Be$

where g_0 = observed gravity; γ_0 = theoretical gravity; Fe = free-air effect; Be = Bouguer effect.

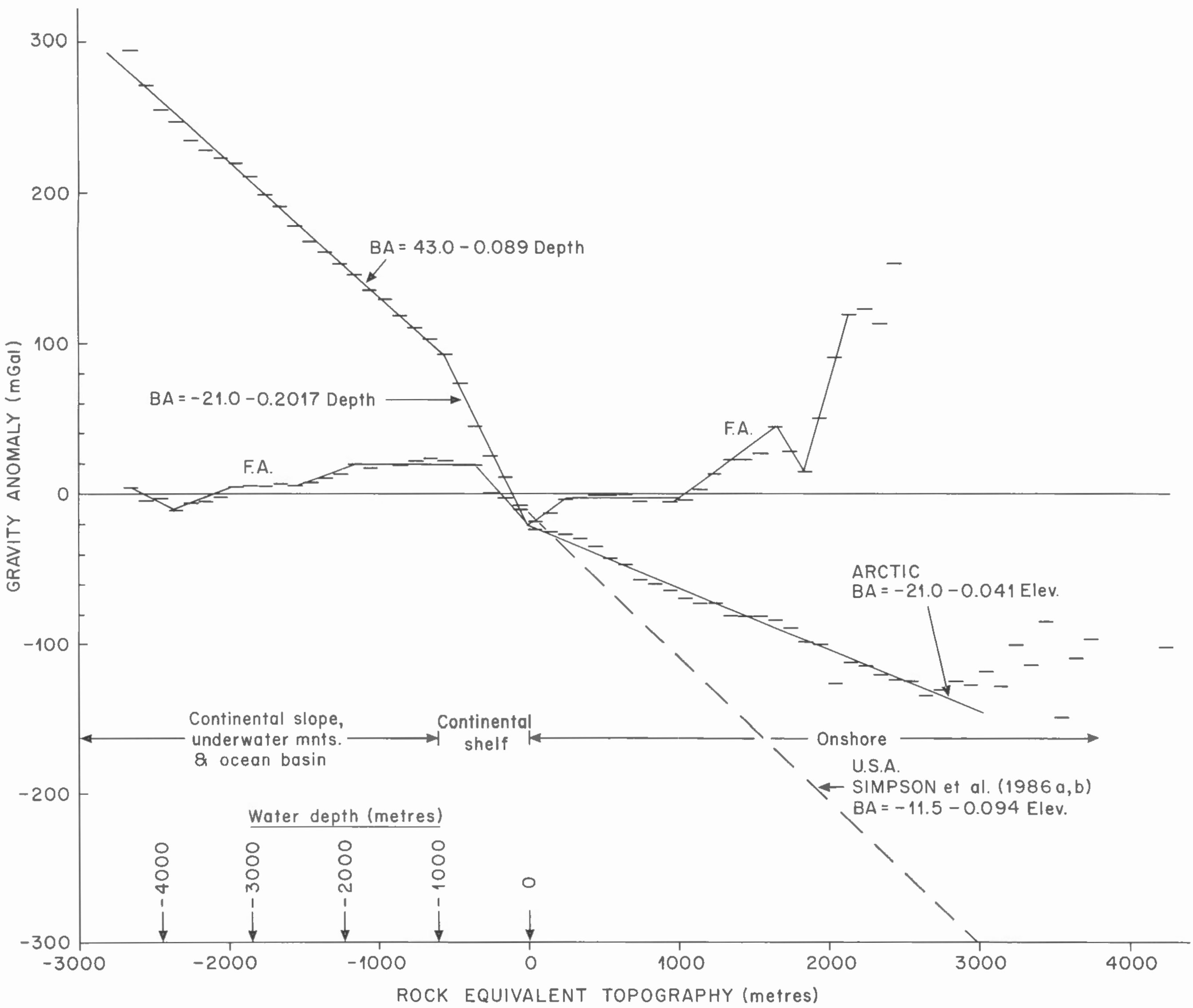

Figure 1. Correlations between average free-air (F.A.) and average Bouguer (BA) anomalies (mGal) and 100 m increments of heights or depths of equivalent rock topography (metres) are shown. Onshore, equivalent rock topography equals the height of land above sea level, except for ice-covered areas of Greenland where the ice (density 0.9 Mg/m^3) is converted to a mass of rock equivalent density of 2.67 Mg/m^3 and added to the height of land. Offshore, water with a density of 1.03 Mg/m^3 is replaced by an equivalent rock topography of density 2.67 Mg/m^3 and depths are given to this rock equivalent surface. Regression lines $y = a+bx$ are shown for Bouguer anomalies for three areas with distinct slopes namely: onshore, $a = -21.0$ and $b = -0.0413$; continental shelf, $a = -21.0$ and $b = -0.2017$; and continental slope and ocean basin, $a = -43.0$ and $b = -0.0890$. For comparison, the regression line for the land conterminous United States taken from Simpson et al. (1986a) is shown for which $a = -11.5$ and $b = -0.0942$.

Observed gravity (g_0) is the value of gravity determined at some field station with respect to a control station. The control station values are based on the International Gravity Standardization Net 1971 (IGSN 71, Morelli et al., 1974). Theoretical gravity (γ_0) which is a function of latitude (Φ) is based on the Geodetic Reference System 1967 (GRS67, International Association of Geodesy 1971) reference ellipsoid where:

$$\gamma_0 = 978.03185\,(1 + 0.005278895 \sin^2 \Phi + 0.000023462 \sin^4 \Phi) \text{ Gal.}$$

One Gal is a unit of acceleration equal to 1 cm/s^2. One mGal is a thousandth of a Gal or equal to 10 μm/s^2.

The free-air effect (Fe) is a function of the elevation or depth of the observed station above or below the reference ellipsoid, respectively, which is taken here as mean sea level.

$Fe = (dg/dz)h - (dg/dz - 4\pi G\rho_w)d_w$ where dg/dz is the vertical gradient of gravity equal to 0.3086 mGal/m, h is the station elevation in metres, G the universal constant of gravitation (6.672×10^{-8}m^3 /Mgs^2), ρ_w the density of sea water (1.03 Mg/m^3), and d_w the depth of water for underwater stations only. The Bouguer effect (Be) is a function of the mass above or below the reference ellipsoid. The usual correction for mass, approximately a semi-infinite flat slab whose top and bottom coincides with the station and sea level, respectively, is

$$Be = 2\pi G\rho_c h + 2\pi G(\rho_c - \rho_w)d_w + 2\pi G(\rho_c - \rho_i)d_i$$

where $2\pi G = 0.04192 \times 10^{-5}$m^3/Mgs^2, ρ_c is the assumed surface crustal density (2.67 Mg/m^3), ρ_i is the assumed density of ice (0.9 Mg/m^3) and d_i is the thickness of ice in metres. Terrain corrections (to account for topographic relief not included in the slab approximation) were made only in the Richardson Mountains.

The various types of gravity anomalies were compared with *rock equivalent topography* to determine the degree of correlation. Rock equivalent topography is obtained by replacing ice or water, where present, by an equivalent mass of rock, density 2.67 g/cm^3, and adding the corresponding rock thickness to the existing topography on land or to the seabottom over the oceans. Mean gravity anomaly values were computed for successive intervals of 100 m elevation, usually containing between 50 and 14 000 gravity observations and plotted against the interval.

Figure 1 shows that the Bouguer anomaly has a strong correlation with elevation, whereas the free-air anomaly has a much more variable and weaker correlation (Sobczak and Halpenny, in press). The free-air anomaly, derived by applying only one elevation-dependant correction (free-air correction) to the original observations, usually is very sensitive to local topography, being relatively positive over local peaks and negative in valleys. Regional topography, however, is generally isostatically compensated and tends to produce a regional free-air field with close to zero values. The Bouguer anomaly, in addition to including the free-air correction, contains a negative correction for the mass or rock above sea level (and a positive correction converting water into rock density 2.67 Mg/m^3 where a water layer is present). As a result, much stronger relationships between Bouguer anomaly and topography were observed. The correlation is related to isostatic compensation at the crust-mantle interface where crustal roots are developed in response to topographic loads.

Compensation concepts (called isostasy) were introduced by Airy (1855) and Pratt (1855). The Airy hypothesis proposed that crustal loads are compensated by crustal roots in much the same way as an iceberg floating in water, whereas the Pratt hypothesis advocated compensation by lateral variations of density within the crust which maintain constant columnar mass down to some equilibrium level. Simpson et al. (1986a, b) and Goodacre et al. (1987) used the Airy model to determine the gravity effect of isostasy. The Goodacre et al. method, used here, concentrates the compensating masses into a thin layer at a depth of 30 km. The gravity effect for these masses is computed over the whole area on a regular grid and is known as the total isostatic anomaly field.

TOTAL ISOSTATIC ANOMALY CORRECTIONS

The merits and variabilities of isostatic correction have been discussed by various authors and are summarized by Simpson et al. (1986a, b). They conclude that the differences in isostatic corrections produced by various models, including the omission of crustal lithospheric strength in distributing compensation, tend to be a small percentage of the total isostatic correction. Here, the elastic parameters of the crust are ignored, the surface topography is reduced to an equivalent layer of rock of density (ρ_c) 2.67 Mg/m^3 and the water layer with a density (ρ_w) of 1.03 Mg/m^3 is condensed to a layer of rock such that $WD \times \rho_w = \rho_c \times ER$, where WD is the water depth and ER is the equivalent rock thickness. The depth to the top of this ER is equal to WD - ER = 0.61423 WD. This rock equivalent topography is placed at a depth of 30 km as a compensating mass and its gravity effect at each grid point is calculated using a weighting function

$$w(r,z) = \frac{1}{2\pi} \left[\frac{z}{(z^2 + r^2)^{\frac{3}{2}}} \right]$$

where z is the depth of compensation and r is the horizontal projection of the distance from the point of compensation to the point being calculated. This weighting is carried out to a distance of 166.7 km. Additional isostatic compensation corrections for the Earth's topography beyond this distance to 180° on a spherical Earth were taken from charts published by Karki et al. (1961). The total isostatic anomaly correction (TIA) at each grid point is equal to

$$TIA = 2\pi G \sum_i h_i \rho_c [w_i(r_i, z)] + KC$$

where KC is the Karki correction and h_i is the elevation in the i^{th} block.

The topography and bathymetry have been gridded at five minute intervals (digitized bathymetric data base, DBDB-5 file) by Francis L. Marchant, Robert R. Murchison, Frederich H. Sorensen, Laverne W. Snodgrass, Oscar B. Eckhoff and Thomas M. Davis of the Bathymetry Division of the United States Naval Oceanographic Office, Stennis Space Centre, Mississippi. The bathymetry corresponds to the GEBCO 5.17 map (Johnson et al., 1979). There was some thought given to digitizing the Perry et al. (1986) map for increased accuracy, but the differences between the two maps for the purpose of computing a total isostatic anomaly correction map, were considered too insignificant to warrant the additional commitment. Thus the DBDB-5 file was used for calculating a rock equivalent topography map used to calculate total isostatic anomaly corrections, although Perry et al. (1986) bathymetry contours are shown on these maps.

The topography of the DBDB-5 file for the Greenland area was modified to accommodate the extensive and very thick (up to 3 km) icecap with an ice density ρ_i equal to 0.9 Mg/m^3. The ice thickness data are from radar-determined, ice-thickness maps provided by the Geodetic Institute of Denmark (Overgaard, 1983). No corrections were made for smaller ice caps such as on Ellesmere and Baffin islands.

Total isostatic anomaly corrections are in excess of 100 mGal over mountainous areas and below −200 mGal over oceanic areas, more or less equivalent in regional magnitudes but opposite in sign to the Bouguer anomaly. The total isostatic anomaly corrections may contain small (<5 mGal, Simpson et al., 1986a), long-wavelength errors for land areas caused by using model parameters different to those used by Karki et al. (1961): Karki et al. used a sea level crustal compensation depth of 30 km and a density contrast of 0.6 Mg/m^3 at the crust-mantle boundary, whereas in the present computations 30 km and 0.4 Mg/m^3 respectively, were used. For the deepest parts of the ocean, these errors may reach 10 mGal (Simpson et al., 1986a). Fortunately, these errors are usually only a small percentage of the large gravity values obtained for Bouguer anomaly and total isostatic anomaly corrections and do not seriously impair the accuracy of these corrections.

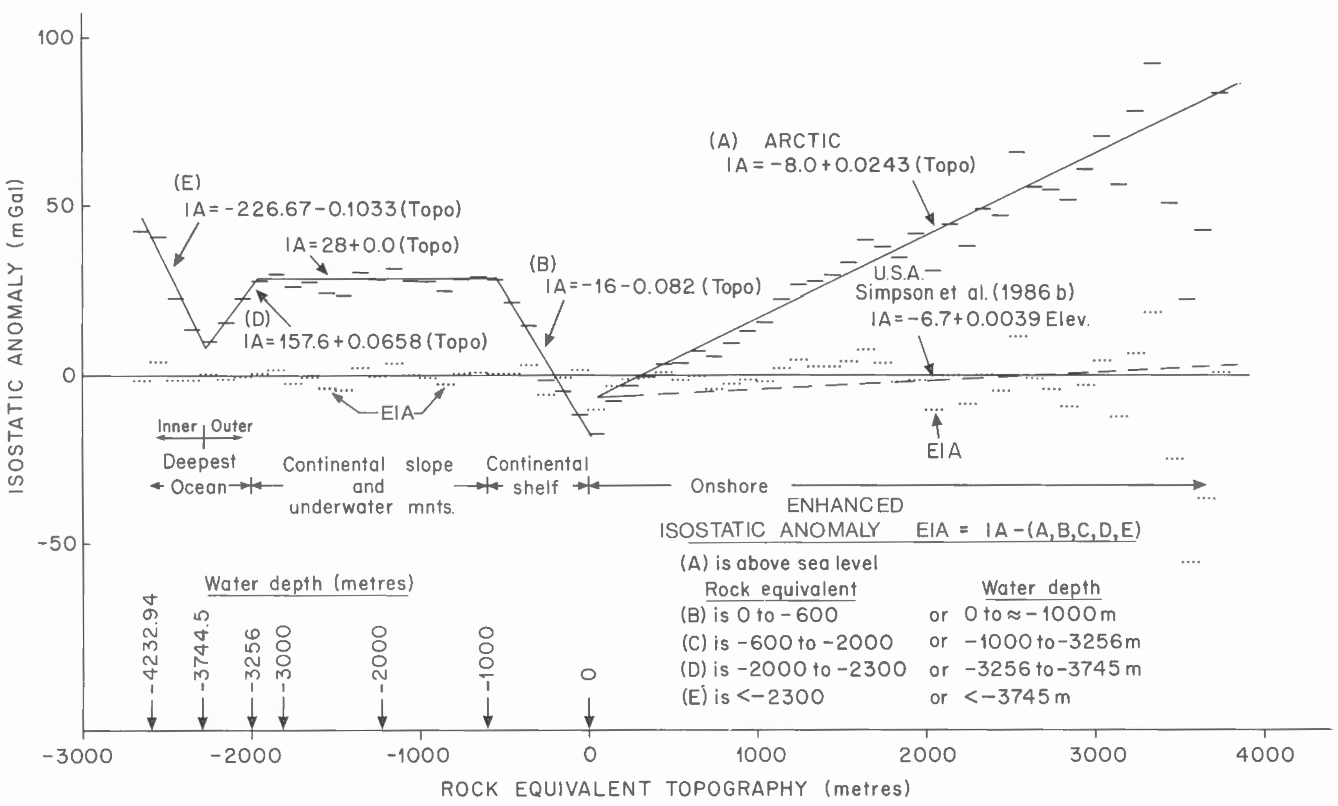

Figure 2. Average isostatic anomalies (IA) versus increments of 100 m rock equivalent topography (elevation and water depths modified). Water depths (m) are also shown for easier comparisons. Regression lines $y = a+bx$ are shown for five areas with distinct slopes namely: onshore, $a = -8.0$ and $b = 0.0243$; continental shelf, $a = -16$ and $b = -0.082$; continental slope and ocean basin, $a = 28$ and $b = 0.0$; and in the central ocean two regression lines with reverse slopes, one for the outer ocean, $a = 157.6$ and $b = +0.0658$ and one for the inner ocean, $a = -226.7$ and $b = -0.1033$. For comparison, the regression line for the United States (taken from Simpson et al., 1986a) is also shown, $a = -6.7$ and $b = 0.0039$. The enhanced isostatic anomaly (EIA) is equal to the isostatic anomaly (IA) minus the appropriate relationship between isostatic anomalies and rock equivalent topography.

ISOSTATIC ANOMALIES

Isostatic anomalies (IA) are equivalent to the sum of the Bouguer anomaly and the total isostatic anomaly corrections; that is, IA = BA + TIA corrections. Removal of the total isostatic anomaly, theoretically, corrects for isostatic distortions in the gravity field, thus an isostatic anomaly map portrays essentially those anomalous areas related to intra-crustal structure. The isostatic anomaly map, in general, bears a resemblance to the combined Bouguer anomaly (land)-free-air anomaly (ocean) map shown by Sobczak et al. (in press).

The Isostatic anomaly map should be used with some caution. Anomalies on this map may be attributed to anomalous mass zones or to areas which are undercompensated or overcompensated.

Isostatic anomalies have a distinct advantage over either Bouguer or free-air anomaly maps in that no anomalies should overcompensate for topography or bathymetry, because the Bouguer correction, if appropriate densities are used, will correct for the topography or bathymetry and the total isostatic correction will correct for the attraction of the underlying compensating masses. However, all loads within the crust below sea level, even if isostatically compensated, may still produce significant isostatic anomalies, as observed in Figure 3. If they were not compensated, the isostatic anomalies would be even larger. Usually, in the absence of knowledge of crustal thicknesses, especially for loads in excess of 100 km in width, it is impossible to tell from gravity how much compensation has taken place. But where thicknesses are known from independent sources an estimation of the degree of compensation may be attempted. For example, the gravity effect (up to 140 mGal) of the mass deficiency of the sediments in the extensive Sverdrup Basin (geometry of sediments determined seismically and from drillholes) is nearly completely removed by isostatic compensation (Sobczak et al., 1986).

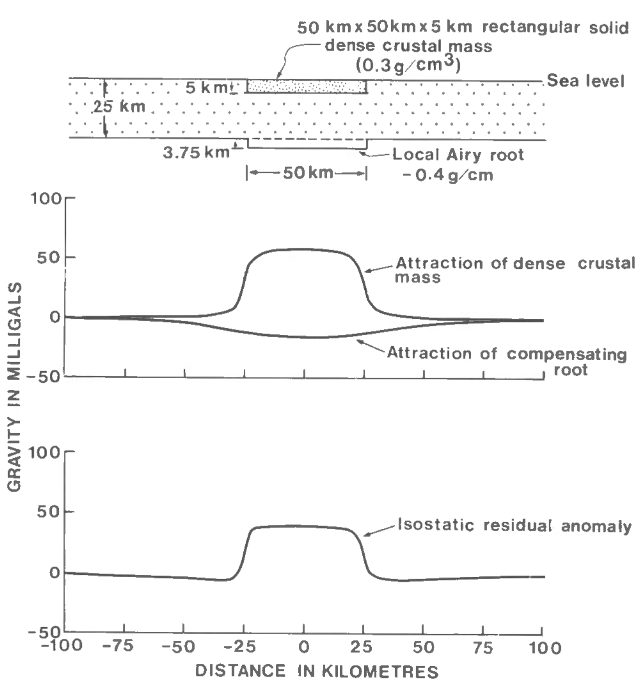

Figure 3. A large, nonzero isostatic anomaly for a dense shallow rectangular mass below sea level which is completely compensated by an Airy deep root (taken from Simpson et al., 1986a).

Average isostatic anomalies were plotted as a function of the rock equivalent topography over land and ocean in increments of 100 m (Fig. 2). Onshore, a regression line ($y = a + bx$) where $a = -8.0$ mGal and $b = +0.0243$ mGal/m shows that the average isostatic anomalies have a positive, uniform correlation with elevation which is much larger than the one obtained by Simpson et al. (1986b) for the conterminous United States where $a = -6.7$ mGal and $b = +0.0039$ mGal/m. This positive relationship suggests that the topography in the Arctic may be adjusting. Probably the upper mantle is buoyed up by a hotter than normal mantle which supports the surface topography. As the mantle cools crustal roots will develop as the crust sinks and the gravity anomalies will tend towards zero as shown by Simpson et al. (1986a).

Over the ocean area, four distinct relationships between isostatic anomalies and water depth were found. In the continental shelf region $a = -16$ mGal and $b = -0.082$ mGal/m; this inverse relationship shows that the isostatic anomaly increases with depth. This region probably reflects a transition zone between an area affected by glacial loading outlined by negative isostatic anomalies to one where oceanic crust is underlain by relatively hot mantle which keeps it elevated giving rise to positive anomalies. As this region cools the mantle will subside and the general level of the positive isostatic gravity anomalies will gradually approach zero.

The continental slope and ocean basin region, where water depths vary from about 1000 to 3300 m, are associated with a flat regression line with $a = 28$ mGal and b is zero. This shows that no relationship exists between water depth and isostatic anomalies. The anomalies are, however, 28 mGal higher than expected. Probably, the upper mantle is still relatively hot and is closer to the surface than if it was cooler. Presumably as the mantle cools it will sink and the gravity anomaly level will decrease to zero.

For ocean depths greater than 3300 m, positive and negative relationships were found for an outer (3300 to 3700 m) and inner (>3700 m) deepest ocean; the outer ocean has a regression line with $a = 157.6$ mGal and $b = +0.066$ mGal/m and the inner ocean has one with $a = -226.7$ mGal and $b = -0.1033$ mGal/m. These relationships intersect at a value of about +7 mGal in the central region of the abyssal plains suggesting that these regions are cooling and sinking, thus lowering the gravity values.

ENHANCED ISOSTATIC ANOMALIES

Isostatic anomalies represent anomalies with a first order isostatic correction for compensating masses to topography and bathymetry, whether this compensation has taken place or not. These anomalies include gravity effects related to other causes such as age, heat balance and large intracrustal density contrasts which also may have an influence on isostasy. Various linear relationships between anomalies and elevation or water depth may still exist (Fig. 2). These regional effects disturb the local gravity anomalies which are usually the subject of discussion and may be removed from the isostatic anomalies using the relationships between isostatic anomalies and topography/bathymetry (Fig. 2). This final correction produces a resultant anomaly provisionally named the enhanced isostatic anomaly (EIA); EIA = IA − R, where R is the regional relationship (linear regression lines, as shown in Fig. 2). Enhanced isostatic anomaly maps should not contain regional effects related to compensatory mechanisms reacting to topographic/bathymetric loads/antiloads or possible thermal buoyancy. The enhanced isostatic anomalies should be directly related to anomalous masses within the crust.

The enhanced isostatic anomaly map, within the limits of accuracy (usually <10 mGal) of the gravity observations and the development of isostatic anomalies, delineates areas of anomalous masses unrelated to topography, edge, boundary, isostatic and regional effects as described above. The zero anomaly contour in this map, shown also in Figure 4, generally coincides with the edges

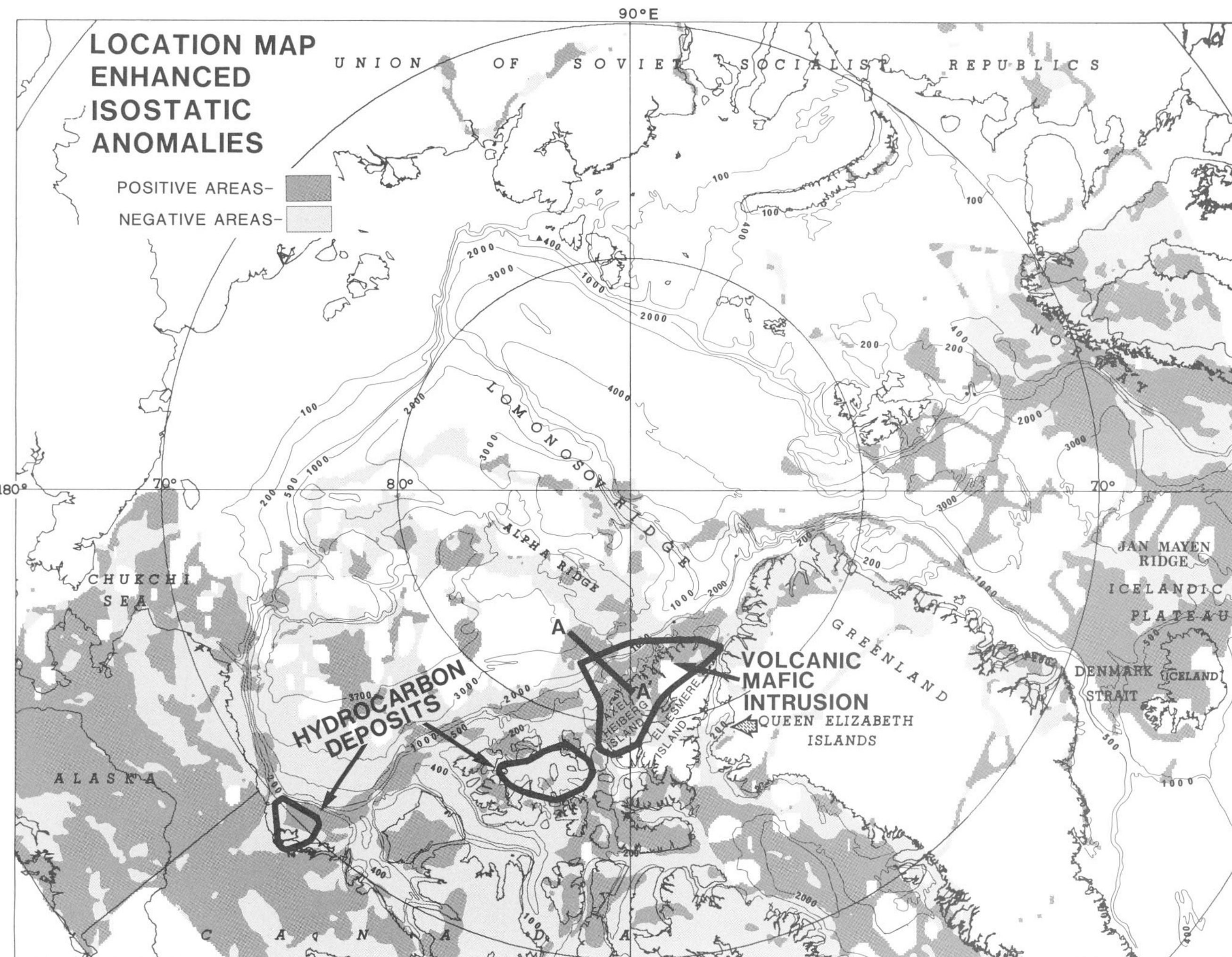

Figure 4. Zero contour lines taken from the enhanced isostatic anomaly map generally correspond with the edges of anomalous masses. Positive and negative areas are indicated. The locations of seven drillholes in and near the area of volcanism in the north-central Queen Elizabeth Islands are shown, as are oceanic crust and location of a profile over Baffin Bay taken from Menzies (1982), and drillhole, continent-ocean boundary and location of a profile over the North Atlantic Ocean from the Voring Plateau to the Jan Mayen Ridge taken from Skogseid and Eldholm (1987). These features are discussed by Sobczak and Halpenny (in press).

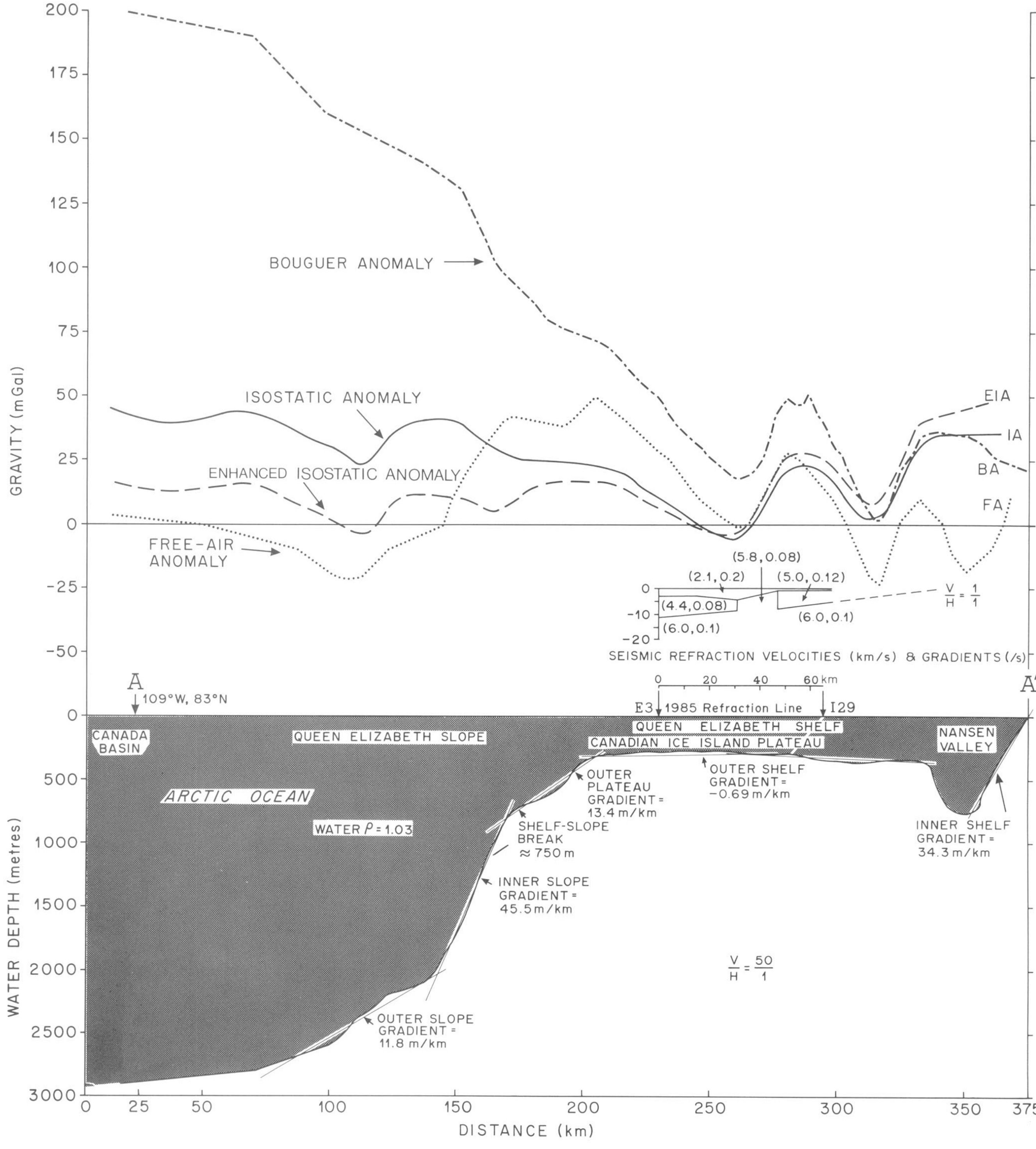

Figure 5. Profile A-A' (Fig. 4) across the Canadian polar margin showing bathymetry, free-air, Bouguer, isostatic and enhanced isostatic anomalies.

of anomalous masses. Three areas (north-central Queen Elizabeth Islands, Baffin Bay and the North Atlantic Ocean) have been discussed briefly with respect to lithology and structure by Sobczak and Halpenny (in press). Figure 5 presents an example of how the different types of anomalies vary across the Canadian polar margin.

SUMMARY

Analyses of the free-air, Bouguer, and isostatic anomalies show distinct relationships with elevations. These relationships were removed to establish a new type of gravity anomaly map - an enhanced isostatic anomaly map. These various types of anomalies are compared in Figure 5 along a profile across the Canadian polar margin to demonstrate some of the shortcomings of the free-air, Bouguer, and isostatic anomalies and the strength of the enhanced isostatic anomalies. Computation of enhanced isostatic anomalies allows us to determine a regional (relationships in Fig. 2) component which can be attributed to thermal conditions in areas of gravity highs and glacial loading effects in areas of gravity lows and a local component which readily delineates the anomalous parts of the crust.

The enhanced isostatic gravity anomaly map nullifies the topography, edge, boundary, isostatic, thermal and glacial loading effects. As a result, the anomalous zones in the gravity field relating to geological structure are more accurately defined because the regional components have been removed. This map outlines areas of older or newer oceanic and continental crust and of stable or unstable crust. Areas that are positive may represent areas of volcanism, intrusion, recent mountain building, and oceanic and transitional crust. Areas with negative anomalies represent either continental crust which has not been activated in the last 100 Ma or so, or oceanic crust which is probably older than 100 Ma. As the oceanic crust gets older the gravity anomalies on the enhanced isostatic anomaly map tend to approach zero, probably indicating that the crust and underlying mantle is gradually cooling and sinking while the whole system is in continuous isostatic equilibrium.

The use of enhanced isostatic anomalies facilitates the investigation of the gravity field along the polar margin. The margin off Axel Heiberg and Ellesmere islands, where detailed seismic refraction lines have been surveyed from the Canadian ice island, is an example of one region which will benefit from examination using the new enhanced isostatic anomalies. In the Queen Elizabeth Islands, the enhanced isostatic anomaly map outlines positive anomalous areas related to metamorphism and volcanism, whereas negative areas are related to sedimentation that may correspond to areas of hydrocarbon potential. For example, a hydrocarbon-rich province in the western Queen Elizabeth Islands, outlined by Nassichuk (1987), corresponds to an area of negative enhanced isostatic anomalies. Similar prospects may be located in other areas of the Arctic using an enhanced isostatic anomaly map.

This analysis has shown that the Arctic, north of 64°N latitude, may be in isostatic equilibrium but is probably still thermally and glacially affected. Extensive areas may still be relatively hot with mantle material buoyed up to account for the regional positive isostatic anomalies and enhanced isostatic anomalies. Also, smaller areas in the Arctic and much larger areas in central Canada may be affected by glacial loading where regional negative isostatic anomalies occur. Locally in the central part of the abyssal plains of the deep ocean, cooling conditions are probaly taking place as the gravity anomalies are lowered to a mean value of +7 mGal. Nearshore, between 300 m water depth and 300 m land elevation (Fig. 2) this area has been overcompensated (enhanced isostatic anomalies down to −18 mGal at the shoreline) due to the residual effect from glaciation, that is ice has loaded the crust and forced it into the mantle giving rise to a crustal root which has supported the ice load. Then when the ice melted, probably quite quickly, the root remained in large part, giving rise to a negative gravity anomaly. Probably, the crust will rise even farther than it has to date (Farrand and Gajda, 1962) to re-establish isostatic equilibrium.

REFERENCES

Airy, G.B.
1855: On the computation of the effect of the attraction of the mountain-masses, as disturbing the apparent astronomical latitude of stations in geodetic surveys; Royal Society of London, Philosophical Transactions, v. 145, p. 101-104.

Farrand, W.R. and Gajda, R.T.
1962: Isobases on the Wisconsin marine limit in Canada; Geophysical Bulletin No. 17, Department of Mines and Technical Surveys, Ottawa, Canada, p. 5-22.

International Association of Geodesy
1971: Geodetic Reference System 1967 Paris; The International Association of Geodesy Special Publication No. 3, 116 p.

Goodacre, A.K., Grieve, R.A.F., and Halpenny, J.F.
1987: Isostatic gravity anomaly map of Canada; Geological Survey of Canada, Canadian Geophysical Atlas, Map 4, scale 1:10 000 000.

Johnson, G.L., Monahan, D., Gronlie, G., and Sobczak, L.W.
1979: General bathymetric chart of the oceans, Arctic Ocean, Chart 5.17; Canadian Hydrographic Service, Ottawa, Canada.

Karki, P., Kivioja, L. and Heiskanen, W.A.
1961: Topographic-isostatic reduction maps for the world for the Hayford zones 18-1, Airy-Heiskanen system, T = 30 km; Publications of the Isostatic Institute of the International Association of Geodesy, No. 35, 23p.

Menzies, A.W.
1982: Crustal history and basin development of Baffin Bay *in* Nares Strait and the drift of Greenland: a conflict in plate tectonics, edited by P.R. Dawes and J. Wm. Kerr; Meddelelser om Gronland, Geoscience, v. 8, p. 295-312.

Morelli, C., Gantar, C., Honkasalo, T., McConnell, R.K., Tanner, J.G., Szabo, B., Uotila, U., and Whalen, C.T.
1974: The international gravity standardization net 1971 (IGSN 71); The International Association of Geodesy, Special Publication No. 4, 194 p.

Nassichuk, W.W.
1987: Forty years of northern non-renewable natural resource development; Arctic v. 40, p. 274-284.

Overgaard, S.
1983: Unpublished maps of the Greenland ice sheet; Electromagnetic Institute, Technical University of Copenhagen, scale 1:2 500 000.

Perry, R.K., Fleming, H.S., Weber, J.R., Kristoffersen, Y., Hall, J.K., Grantz, A., Johnson, G.L., Cherkis, N.Z., and Larsen, B.
1986: Bathymetry of the Arctic Ocean; Williams and Heintz Map Corporation, Capital Heights, MD. 20743, Map and Chart Series MC-6.

Pratt, J.H.
1855: On the attraction of the Himalaya Mountains, and of the elevated regions beyond them upon the plumb-line in India; Royal Society London, Philosophical Transactions, v. 145, p. 53-100.

Simpson, R.W., Jachens, R.C., and Blakely, R.J.
1986a: A new isostatic gravity map of the conterminous United States with a discussion on the significance of isostatic anomalies; Journal of Geophysical Research, v. 91, p. 8348-8372.

Simpson, R.W., Jachens, R.C., Saltus, R.W., and Blakely, R.J.
1986b: Isostatic gravity, topographic, and first-vertical-derivative gravity maps of the conterminous United States; United States Geological Survey, Map GP-975.

Skogseid, J. and Eldholm, O.
1987: Early Cenozoic crust at the Norwegian continental margin and the conjugate Jan Mayen Ridge; Journal of Geophysical Research, v. 92, p. 11471-11491.

Sobczak, L.W., Mayr, U., and Sweeney, J.F.
1986: Crustal section across the polar continent-ocean transition in Canada; Canadian Journal of Earth Sciences, v. 23. p. 608-621.

Sobczak, L.W., Hearty, D.B., Forsberg, R., Kristoffersen, Y., Eldholm, O., and May, S.P.
In press: Gravity from 64°N to the North Pole, *in* The Arctic region, edited by A. Grantz, L. Johnson, and J.F. Sweeney; Geological Society of America, The Geology of North America, v. L.

Sobczak, L.W. and Halpenny, J.F.
In press: Gravity anomaly maps of the Arctic (Free-air, Bouguer, isostatic and enhanced isostatic); Tectonophysics, Special issue.